Scientific Research Publishing

American Journal of Analytical Chemistry, 2023, 14, 28-54
https://www.scirp.org/journal/ajac
ISSN Online: 2156-8278
ISSN Print: 2156-8251

Revisiting "Non-Thermal" Batch Microwave Oven Inactivation of Microorganisms

Victor John Law*, Denis Pius Dowling

School of Mechanical and Materials Engineering, University College Dublin, Dublin, Ireland
Email: *viclaw66@gmail.com

How to cite this paper: Law, V.J. and Dowling, D.P. (2023) Revisiting "Non-Thermal" Batch Microwave Oven Inactivation of Microorganisms. *American Journal of Analytical Chemistry*, **14**, 28-54.
https://doi.org/10.4236/ajac.2022.141003

Received: November 30, 2022
Accepted: January 16, 2023
Published: January 19, 2023

Abstract

Over the last few decades there has been active discussion concerning the mechanisms involved in "non-thermal" microwave-assisted inactivation of microorganisms. This work presents a novel non-invasive acoustic measurement of a domestic microwave oven cavity-magnetron operating at f_o = 2.45 ± 0.05 GHz (λ_o ~ 12.2 cm) that is modulated in the time-domain (0 to 2 minutes). The measurements reveal the cavity-magnetron cathode filament cold-start warm-up period and the pulse width modulation periods (time-on time-off and base-time period, where time-on minus base-time = duty cycle). The waveform information is used to reconstruct historical microwave "non-thermal" homogeneous microorganism inactivation experiments: where tap-water is used to mimic the microorganism suspension; and ice, crushed ice, and ice slurry mixture are used as the cooling media. The experiments are described using text, diagrams, and photographs. Four key experimental parameters are indentified that influence the suspension time-dependent temperature profile. First, where the selected process time > the time-base, the cavity-magnetron continuous wave rated power should be used for each second of microwave illumination. Second, external crushed ice and ice slurry baths induce different cooling profiles due to difference in their heat absorption rates. In addition external baths may shield the suspension resulting in a retarding of the time-dependent heating profile. Third, internal cooling systems dictate that the suspension is directly exposed to microwave illumination due to the absence of surrounding ice volume. Fourth, four separated water dummy-loads isolate and control thermal heat transfer (conduction) to and from the suspension, thereby diverting a portion of the microwave power away from the suspension. Energy phase-space projections were used to compare the "non-thermal" energy densities of 0.03 to 0.1 kJ·m^{-1} at 800 W with reported thermal microwave-assisted microorganism inactivation energy densities of 0.5 to 5 kJ·m^{-1} at 1050 ± 50 W. Estimations of the "non-thermal" microwave-

assisted root mean square of the electric field strength are found to be in the range of 22 to 41.2 $V \cdot m^{-1}$ for 800 W.

Keywords

Thermal, Non-Thermal, Microwave-Assisted, Microwave Oven, Acoustic, Food, Microorganisms

1. Introduction

The first US pattern for reheating of foodstuff in a multimode microwave oven was filed in 1945 [1]. Today's domestic multimode microwave ovens use a free-running cavity-magnetron operating a frequency of f_o = 2.45 ± 0.05 GHz (free space wavelength, λ_o ~ 12.2 cm) as the energy source. At this frequency, the microwave photons have insufficient energy to break molecular bonds and for this reason the electromagnetic radiation is considered to be non-ionizing [2] [3] [4]. However, bio-materials (carbohydrate, protein, and vitamin and enzymes) placed within a microwave electromagnetic field undergo a rapidly changing complex permittivity ($\varepsilon^* = \varepsilon' - j\varepsilon''$) that is thought to induce translational and rotational motion effects [3] [4] [5]. Some of the earliest reports of domestic multimode microwave oven use for "non-thermal" microwave-assisted continuous flow treatment of bacteria by Kozempel *et al.* (1998) [6], Kozempel *et al.* (2000) [7], and Shazman *et al.* (2008) [8] in food processing and microbiology journals. Notably, researchers at the Department of Microbiology and Immunology, UBC, Canada have played a major role in the development of batch "non-thermal" microwave-assisted inactivation process, where ice and ice slurry baths are used to regulate the temperature of: bacteriophage Wang *et al.* (2001) [9], Baines (2005), Bryant *et al.* [10] (2007) [11] and; Gram-negative vegetative *E. coli* Barnett *et al.* (2006) [12], and Assay *et al.* (2008) [13]. However, the description of the microwave-assisted cooling baths was brief (66 to 213 words), and without diagrams, or photographs: making it difficult to understand the complexly of the volumetric heating process. In addition, in [6]-[13] microwave assisted treatments, the ambiguous term "non-thermal" or "athermal" began to be used in an attempt to differentiate dielectric volume heating and electrical conductive (Ohmic) heating [14]-[23], from possible direct microwave interaction with specific microorganisms. In the later two references, Hayes (2004) [22] and Hayes and Collins (2005) [23] changed the cooling medium from ice baths to forced air cooling of the outer surface of the reaction vessel in organic and biochemistry synthesis, where the technique is known as enhanced microwave synthesis (EMS), a method that produces higher yields and shorter processing times as compared to classic thermal treatment. The generally accepted view (but still controversial) is that within the microwave irradiation period itself, selective heating of polar and ionic molecules (lipids, proteins, carbohydrates, DNA) within microorganism cytoplasm and cell wall mem-

brane reach a high local instantaneous temperature (T_i) causing specific heat transformations that lead to cell lysis. "Non-thermal" effects (bulk temperature (T_B) at < 40˚C) are claimed to be associated with direct microwave interaction that cause: electroporation [5] [7] [9] [10] [11] [12] [24], cell rupture [7] [9] [10] [11] [13] and disruption at the metabolic and genetic [3] [5] [7]. The obscuring or masking of the underlying "non-thermal" (where $T_B \ll T_i$) by "thermal" effects, both in time and space are thought to occur particularly in continuous liquid flow experiments [6] [7] [8] and continuous aerosol flow [25] [26], or indeed in inorganic chemistry syntheses [3] [22] [23] [27] [28].

Wang *et al.* (2019) [29] demonstrated microwave inactivation of Gram-negative vegetative *E. coli* was more efficient in airborne environments as compared to liquid suspensions. In their conclusion it was considered that volumetric heating was the main mechanism in the liquid suspension phase, whereas microwave photon is able to react directly with vegetative *E. coli*, thereby indicating a "non-thermal" microwave effect.

From 2000, domestic and industrial microwave ovens were employed in batch microwave oven generated steam (MGS) decontamination of N95 respirators that were inoculated with influenza virus and bacteriophage MS2 [30]-[34]. With regard to these batch MGS decontamination studies, two studies by Law and Dowling (2021) [35] [36] were published on thermodynamics and dielectric analysis of the MGS decontamination process. Siddharta *et al.* (2016) [37] also reported on a microwave oven (rated at 800 W continuous wave (CW)) that was employed in the batch microwave-assisted inactivation of the hepatitis C virus (HCV) and human immune deficiency virus (HIV).

For volumetric heating of homogenous dielectric materials, Geedipalli *et al.* (2007) [38] used a physics-based model to map in 4-dimensions (*x, y, z, and t*) batch microwave oven heating uniformity of potato, and Yeong *et al.* (2017) [39] has also used COMSOL software studies for distilled water. Building on this work, Lee *et al.* (2020) [40] used OpenFoam software to reveal that under pulsed modulated conditions (T_{on} = 10 seconds and T_{off} = 20 seconds) an increase in the average water flow velocity in the initial T_{on} period then fluctuates downwards in the following T_{off} period. Similarly the temperature standard deviation rises in the first T_{on} period then steadies in the following T_{off} period. Over the next modulated 60 seconds, the temperature standard deviation increases in a step-like behavior while flow velocity falls in similar step-like behavior. The overall effect is to improve heat uniformity throughout the water volume when compared to CW mode of operation. Therefore, truncating the T_{off} period ($t \to 0$) will induce the CW mode and breakdown heat uniformity. In effect, if heat uniformity is important to the user, the duty-cycle (D) should be used, although a longer microwave irradiation time will be required. From this perspective, pulse modulated operation may induce "non-thermal" microwave transformations in the T_{off} period.

In 2022, four microwave-assisted review articles, with a primary focus on the

removal of harmful microorganisms in food processing and the environment were published. Kubo *et al.* (2022) [41] reviewed microwave (300 MHz to 300 GHz) and Ohmic heating of microorganism, food proteins, and enzymes. The authors rightly discuss the challenges in comparing mono-mode with multi-mode experiments, in particular temperature uniformity within multimode microwave ovens hot spots and temperature profile, and the measurement thereof whilst simultaneously removing heat during the irradiation process. It was noted that the complex heterogeneous nature of food (*i.e.* tomatoes, grapes, and juices etc.) have food elements of dimensional scale that influence the microwave electric field and hence mask "non-thermal" effects. From this perspective simple model systems need to be developed and experiments well documented for reliable conclusion on the expectance and extent of "non-thermal" effects. Similarly, Gut [42] wrote a letter to the editor of Food Chemistry with a Response to "non-thermal" conceptual and methodological problems [43]. In the letter he presents an optimistic and constructive approach to explore "non-thermal" effects in broader range of electric field frequencies and strengths, through experiments or simulations, and to collaborate with the advance of emerging technologies, such as Ohmic and PEF, in the food processing sector. Notable, Zhang *et al.* [44] discussed the possibility of destroying biofilms and antibiotic resistance bacteria by microwave irradiation.

In these publications [41] [42] [43] [44] there was no direct reference to the domestic microwave oven pulsed width modulated (PWM) waveform that controls the power time period (T_{on}) and power off (T_{off}) time periods of the cavity-magnetron, where increasing T_{on} results in a decrease in T_{off}. This is a key aspect of microwave-assisted processing as it provides macro control of the cavity-magnetron applied power that is suitable for heating of foodstuff and water, and less sensitive chemical procedures such as digestion and moisture analysis [23]. This oversight is unfortunate, as it well known that homogeneous microorganism populations follow a first-order rate law inactivation behavior, and a heterogeneous population invariably does not [45]. Given that many historical studies of microwave oven microwave-assisted disruption and inactivation studies of homogeneous bacteria and virus populations [9]-[20] [30]-[34], Law and Dowling (2022) [46] [47] data mined these studies to map the microorganism resilience to microwave stress on to a energy phase-space projection for a specific fomite. The range of fomites being: moist face towels, cotton swabs, kitchen sponge, and scrubbing pad, syringes, and cigarette filters and N95-like respirator. Their results found that in either linear-linear or log-linear projection, the process energy budget (measured in kJ) is plotted on the horizontal axis and the energy density ($kJ \cdot ml^{-1}$) plotted on the vertical axis, while inactivation reduction is compressed to $\geq 4 \log_{10}$. Here, an inactivation reduction of $\geq 4 \log_{10}$ is used as a measure of resilience before the fomite-microorganism system moves into a different region of state space when subjected to stress, Carpenter *et al.* (2001) [48], and Cumming and Coiler (2005) [49]. **Figure 1** shows the results for:

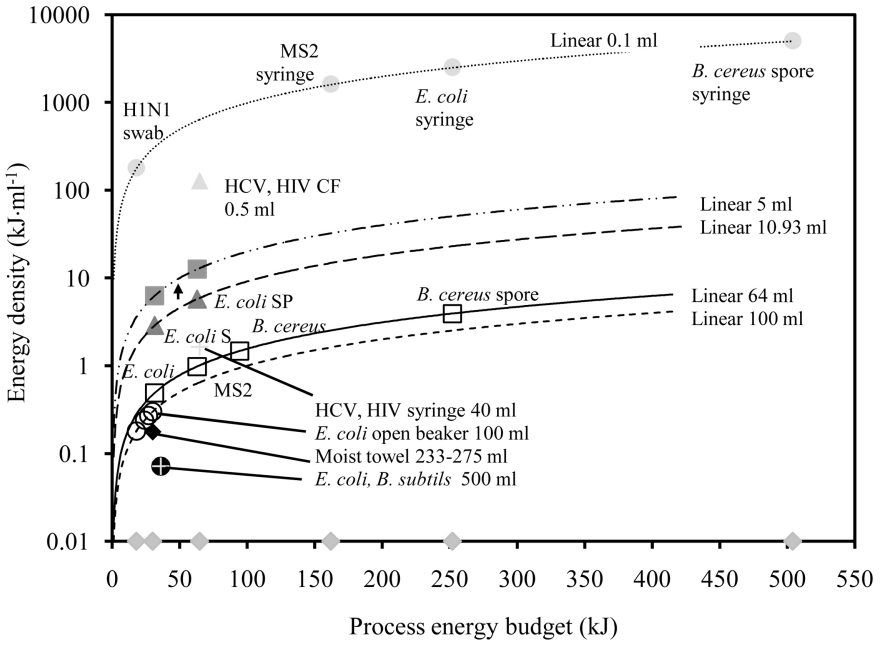

Figure 1. Energy phase-space projection (log-linear) for microwave-assisted ≥4 $\log_{10}$ inactivation of microorganism suspensions within different fomites; *E. coli* beaker 100 ml suspension (open circles), *E. coli* kitchen sponge (S: triangle to square), *E. coli* kitchen scrubbing pad (SP: green triangle to green square), moist towel (black diamond). H1N1 swab, bacteriophage MS2 syringe, Gram-negative vegetative *E. coli* syringe, and *B. cereus* spore on the 0.1 ml iso-volume trend-line (blue square). Spiked (0.5 ml) cigarette filter (CF: blue triangle).

Gram-negative vegetative *E. coli*, Gram-positive *B. cereus*, Gram-positive *B. subtils*, HCV, HIV, and H1N1 for different fomites of varying dielectric properties. The figure reveals that the majority of Gram-negative *E. coli* data points are clustered in the low 20 to 100 kJ process energy budget region, whereas the remaining data points lay along specific volume-trend lines.

Over lapping the publication time period of [46] [47], Su *et al.* (2022) [50] used the specific form of power absorption efficiency (PAE) that equates to the ratio of the power used to heat the material to the input power) to define energy utilization efficiency of microwave oven heating of dielectric porous materials, *i.e.* not-ready-to eat products. In addition, they showed that for binary dielectric materials, relative position and geometry may interfere with and shield the local electromagnetic fields. From this it is reasonable to assume that the baths thermal conduction rate may also be affected. It is self-evident that there are many areas in the research described in [46] [47] [50] overlap and would thus benefit in further development in medium and geometry.

In 2022, Bazana *et al.* [51] published a study on batch thermal microwave-assisted inactivation of *Candida* spp. in a 25 ml agar plated Petri dish. The study used an Electrolux ME28S microwave oven a (rated at 900 W CW, illuminating a 28 L oven cavity [52]) and exposure time of 40 seconds. For this irradiation time, the process energy budget = 36 kJ and energy density = 1.44 kJ·ml^{-1}.

This would indicate that *Candida* spp. in agar suspension has a similar microwave stress behavior to that of Gram-negative vegetative *E. coli* in liquid suspension.

2. The Aim of This Work

The aim of this work is to bring to the attention of American Journal of Analytical Chemistry readers the complex thermal and microwave interaction within "non-thermal" microwave-assisted volumetric heating of ice and ice slurry bath that constitutes a binary dielectric mixture, within multimode microwave ovens. To achieve this objective, the reconstructed experiments are described here using detailed text description, diagrams, and photographs. A non-invasive acoustic recording of the time-modulated cavity-magnetron and its control relays with a 20 liter Bluesky; model BMG20-8, cavity, rated at a 2.45 GHz, 800 W CW is used. This approach enables researchers to characterize the microwave oven applied power with minimum electrical expertise. The measurement technique is combined with standard thermal temperature measurement and calorimetric analysis of "non-thermal" microwave-assisted heating of fixed quantity of tap-water under both internal and external cooling conditions. Section 3 describes the calorimetric and acoustic calibration of the microwave oven. In section 4, this knowledge is use to experimentally compare suspension time-dependent temperature profiles of "non-thermal" microwave-assisted experiments pertaining to bacteriophage [9] [10] [11] and Gram-negative vegetative *E. coli* [12] [13]. In these experiments, a standardized 10 ml of tap-water is used to represent a thermal equilibrated microorganism suspension that is cooled using either an internal ice bath, or external crushed ice or ice slurry bath whilst being microwave irradiated for process times from 0 to 40 s. To separate out thermal heat transfer (conduction) pathways to and from the suspension volume a further set of experiments using four separated water dummy-loads is performed. Section 5 provides an energy phase-space projection and electric field strength analysis of this work. Section 6 provides a summary of the reconstructed "non-thermal" microwave-assisted experimental results and their impact on the historical "non-thermal" microwave-assisted inactivation of microorganism experiments [9]-[13], and outlook for both experiments and simulation.

3. Microwave Power Calibration of a Domestic Microwave Oven

The domestic microwave oven is primarily designed to defrost and heat foodstuff using a free-running cavity-magnetron operating a frequency of $f_0^{'}$ = 2.45 ± 0.05 GHz [1] within a multimode cavity. In many cases of these relatively low cost (60 to 70 euro in 2022) appliances, the cavity-magnetron, and its cathode filament heater, normally employs a Feinberg voltage-doubler drive circuit [53] that is turn-on and turn-off at the step-up side of the microwave oven transformer (MOT) using a PWM circuit. **Figure 2** depicts such a circuit with the position

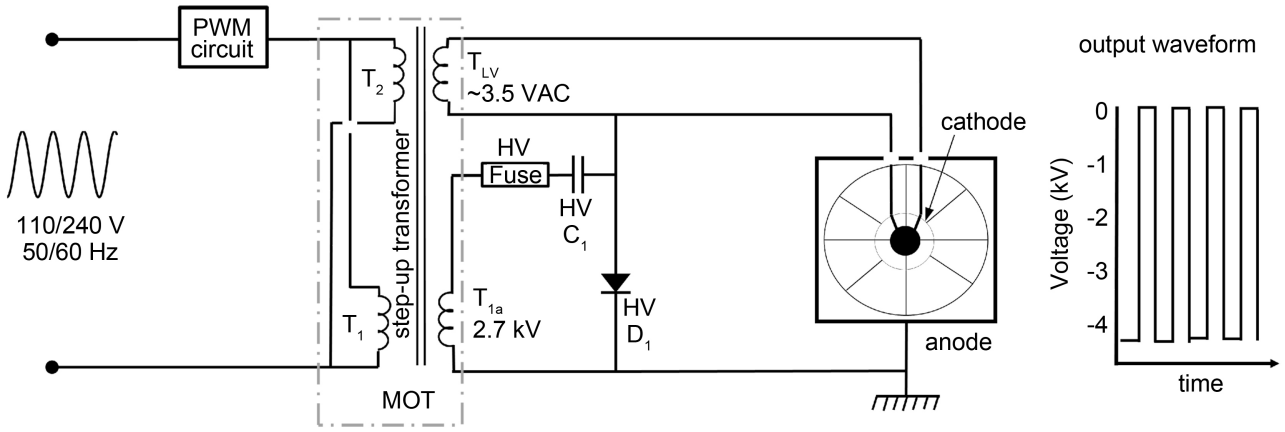

Figure 2. Feinberg voltage-doubler circuit as used in most domestic microwave ovens. Note the position of the PWM circuit board and relay is on the step-up side of the MOT. The right-hand-side of the schematic is shown a typical negative voltage pulse waveform of the cavity-magnetron cathode.

of the PWM circuit board. For further details of this circuit and other cavity-magnetron drive circuits see [54].

3.1. Cavity-Magnetron Applied Power Calibration (Calorimetric)

The microwave energy applied to a multimode cavity is normally calibrated using the calorimetric open water-dish load method [30] [31] [38] [39] [40] [55] [56] [57]. Typically the power calibration is achieved by setting the PWM circuit to CW mode (full power), or a pre-selected D value, then with a dummy-load of 500 to 1000 ml of tap-water in the oven's cavity, the cavity-magnetron is turned on for a pre-selected time. Equation (1) provides the calibration measurement in mathematical terms for the dummy-load.

$$P = mC\frac{\Delta T}{t} \tag{1}$$

where P is rated or applied power (W, or $J{\cdot}s^{-1}$), is the mass (g) of water, C is heat capacity (4.184 $J{\cdot}g^{-1}{\cdot}K^{-1}$) of water, ΔT is the change in water temperature (final temperature minus the initial temperature), and t is the heating time measured in seconds using a stopwatch that is independent of the ovens timing system. For example cavity magnetron rate at 800 W CW will take 261.5 s, (4.35 minutes) to heat 1000 ml of tap-water through a temperature of 20˚C to 70˚C.

3.2. Cavity-Magnetron Calibration (Acoustic)

Acoustic recordings are commonly used to interpret and understand the hidden workings of complex electro-mechanism systems [58], and acoustic string instruments [59]. In this work, acoustic recordings are used to identify the high-voltage relay and MOT noise within the Bluesky microwave oven. The acoustic recordings are made using Audacity® version 2.4.2 (a free, open-source, cross platform audio software) on a Lenovo laptop running Microsoft Windows 10 [59]. The acoustic time-domain waveforms are then analyzed for the high-voltage relay, MOT and cavity-magnetron's cathode filament turn-on and turn-off

for a 500 ml water dummy-load. For the power level description 'medium to lower' used in [12] and 5th level out of 9 levels used in [13], it is reasonable to equate this to the Bluesky microwave oven power level of D = 55%; 440 W, 22 W·L^{-1}.

Figure 3 provides an image of the acoustic a recording for the power level of D = 55% under cavity-magnetron cold-start conditions. The recording reveals within an initial 4 s irregular [54] [60] cathode filament burst followed by a more uniform burst at 8 to 12 s. Secondly, after these two cathode filament heating periods there is a small in amplitude and large in amplitude click. A timestamp analysis of the leading edge of first filament uniform burst and the large acoustic click mathematically corresponds to the T_{on} period and the period between the large acoustic click the leading edge of the second filament uniform burst corresponds the T_{off} period. From this observation the acoustic click may be associated with the high voltage relay turning on, and turning off, and the acoustic bursts are from the cavity-magnetron cathode filament heating period.

Figure 4 provides three aligned and annotated acoustic recordings of the Bluesky oven after the cavity magnetron cathode filament has been heated for 20 s at a power setting of D = 55%. The acoustic recordings are for microwave irradiation time of 85 seconds at D = 33%, 55% and 70%, respectively. Using this format, a number of comparative features can be identified. First, for D = 33%, the recording reveals an initial burst lasting for approximately 4 s followed by reduced noise level lastly approximately another 6 s. Second, within the succeeding section two acoustic clicks are presents followed by a further reduction the noise level. A timestamp analysis of the leading edge of preceding T_{on} period and the second acoustic click mathematically identifies the expected MOT high-voltage relay turn-on (20 ± 0.5 s), and turn-off (30 ± 0.5 s) and a base-time (T_{on} + T_{off}) of 30 ± 0.5 s. Thirdly, similar analysis for D = 55 (middle track) and 70% (lower track) have been performed Table 1. Note however in the lower tack (D = 70%) a warm-up burst appears to be captured which suggest that there is a timing inaccuracy within the PWM board.

Based on the Bluesky oven manufactures manual information, the D calculations yield a time-base of 30 to 31 s. This value is now used to evaluate the

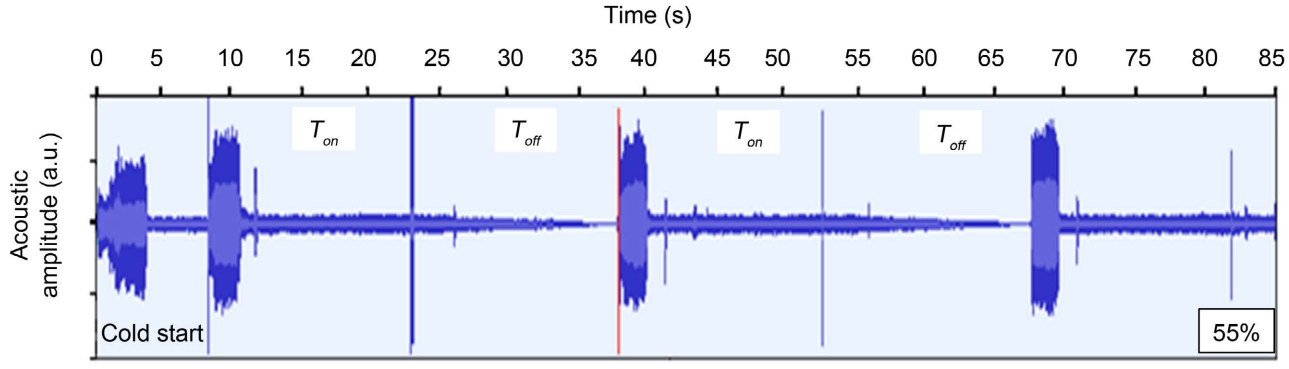

Figure 3. Acoustic recording of the Bluesky microwave oven under cold-start conditions with a 500 ml water dummy-load for a power setting of D = 55%.

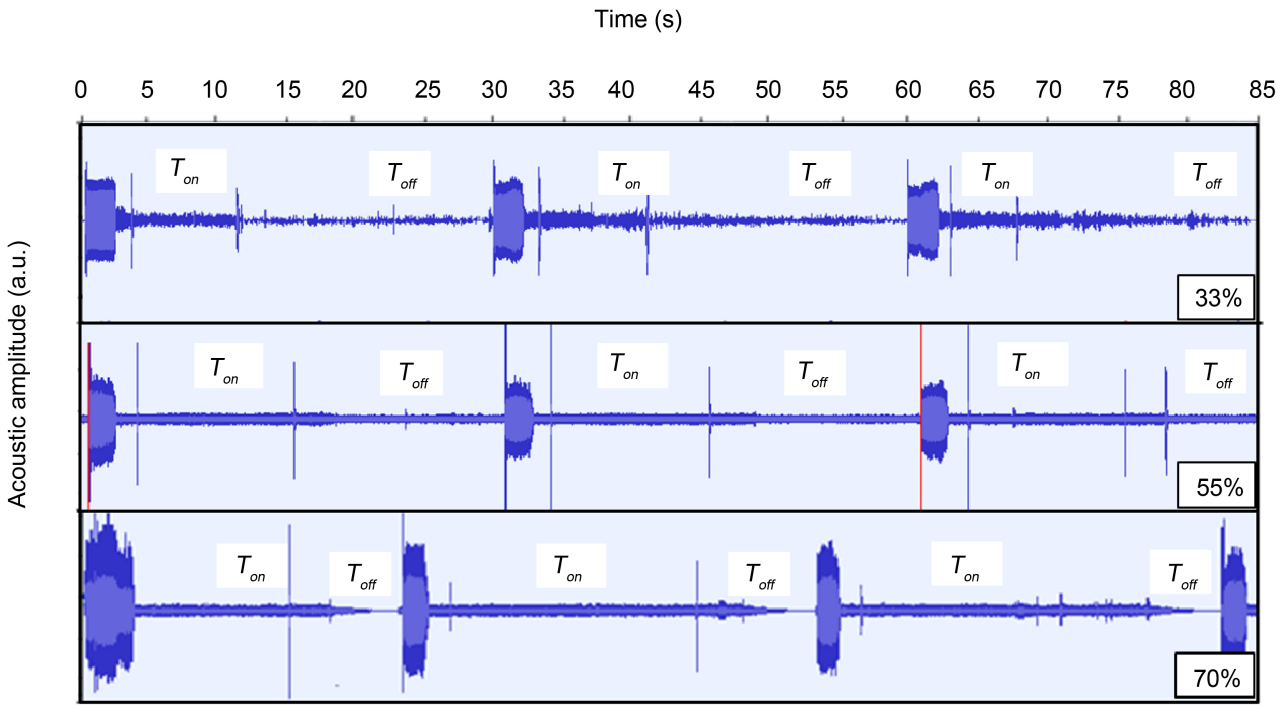

Figure 4. Acoustic recording of the Bluesky microwave oven under warm-up conditions with a 500 ml water dummy-load. Power level: D = 33% (upper track), D = 55% (middle track), and D = 70% (lower track). The back vertical short dashed-line represents the maximum microwave irradiation time used in [12] [13].

Table 1. Bluesky microwave oven manufacture's thermal power specification and acoustic recording timestamp data obtained for T_{on}, T_{off}, base-time period, and computed D values.

Manufactures applied power setting	Measured T_{on} (s)	Measured T_{off} (s)	T_{off} + T_{on} (s)	D (%)
70%, 560 W, 28 W·L^{-1}	~21	~9	30 to 31	~70
55%, 440 W; 22 W·L^{-1}	~16.5	~13	30 to 31	~55
33%, 264 W; 13.2 W·L^{-1}	~11	~20	30 to 31	~33

"non-thermal" microwave-assisted inactivation of microorganism suspension reconstruction of [9]-[13].

4. Internal Ice, and External Ice and Ice Water Bath Microwave-Assisted Time-Domain Temperature Profile Measurements

The centrifuge tube-in-tube system was first used by Wang *et al.* [9] as a cooling mechanism in "non-thermal" microwave-assisted microorganism inactivation experiments; Baines [10] further developed this procedure. In these experiments the internal tube contained solid ice, with the annulus between the tubes containing the microorganism suspension. These systems, however, were found to produce inconsistent microorganism inactivation results due to small quotients of suspension volume and poor thermal contact between the coolant and suspension. Bryant *et al.* [11] and Barnett *et al.* [12] replaced the internal bath for

an external crushed ice bath and increased the suspension size, in doing so improving thermal contact and measurement reproducibility. In the final series of experiments, Asay *et al.* [13] used an external ice water slurry bath to regulate the temperature of an intermediate water bath that was in contact with a Petri dish that contained the microorganism suspension. This complex arrangement is henceforth termed a "double bath system". The five publications [9]-[13] hold a rich source of experimental data spread over three domestic microwave ovens. However as with most experiment parameters reported on similar subject matter by different authors, experimental conditions were not reported in a consistence manner. **Table 2** lists the experimental parameters as reported by the five papers. The: * indicate secondary source information obtained from on-line manuals, and the ** indicates complete information is unavailable. The grey colored cells indicate the need for further experimental measurement investigation.

Table 2. "Non-thermal" microwave oven experimental data for [9] [10] [11] [12] [13].

Microwave oven	Samsung MW5592W [9] [10]	Samsung MW5592W [11]	Panasonic Mn-5853C [12]	Toshiba ER-754BTC [13]
Microorganism (growth temperature)	Bacteriophage T4 and T7 (37˚C)	Bacteriophage T4 (37˚C)	*E. coli C*29 (37˚C)	*E. coli C*29 (10, 26 and 37˚C)
Microwave CW power	1000 W*	1000 W*	800 W	650 W
microwave power setting	Full power	Full power	Medium to low power	5 out of 9 levels
Estimated applied power	1000 W	1000 W	400 W	325 W
Rotating glass carousel	Yes	Yes	Yes	Yes
Oven volume	1 cuft* (28.3 L)	1 cuft* (28.3 L)	Not given	Not given
Ice bath	10 ml frozen ice centrifuge tube**	packed ice in 1 L glass beaker	500 ml glass beaker filled with ice	N/A
Ice water bath	N/A		N/A	Large bucket
suspension vol. and vessel	4 ml in 30 ml centrifuge tube**	0.5 ml in glass Petri dish**	10 ml in 50 ml beaker**	10 ml in Petri dish***
Irradiation time (s)	5, 10, 15, 20, 25	10, 20, 30, 40	15, 20, 25, 30, 35, 40	20, 40
Final suspension temperature	60˚C at 20 s [9] Not given [10]	Not given	29˚C at 40 s	26˚C ± 1˚C

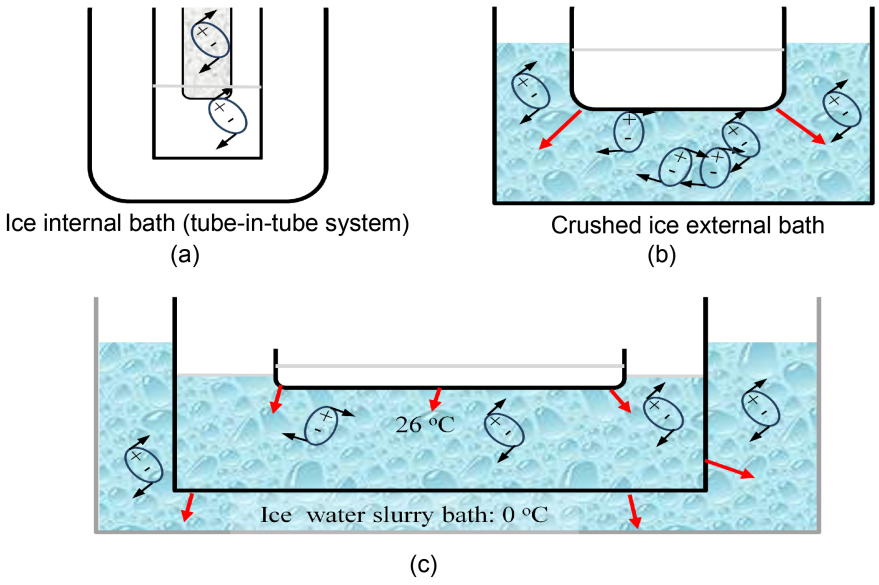

Figure 5. (a) Internal ice bath (tube-in-tube) for "non-thermal" microwave treatment [9] [10]. (b) External crushed ice bath for "non-thermal" microwave treatment using 50 ml beaker [11]. (c) External double bath for "non-thermal" microwave treatment [13]. The rotating ± symbols indicate regions of dielectric volume heating.

4.1. Experiment Reconstruction Methodology

Influenced by the bath design appraisal, three complex load geometries are investigated, see **Figure 5**. These are the tube-in-tube, beaker-in-Petri dish, and the double bath system. To fit within the oven a pseudo-suspension volume of 10 ml with an initial temperature of 37˚C is used. The three cooling experiments performed are: centrifuge tube-in-tube, glass beaker-in-Petri dish, and three Pyrex glass Petri dishes stacked within each other for the intermediate water bath. Ice and crushed ice water volumes used have a characteristic linear scale dimension of $\lambda_m/\lambda_o \sim 0.25$ to 0.5 insuring a microwave standing wave structure is present within the irradiated water volumes. In all of the reconstructions, tap-water is used to mimic the microorganism suspension.

4.1.1. Temperature Measurement

The temperature of ice, crushed ice water slurry bath and pseudo-suspensions and time-course are recorded using a digital thermometer (temperature range −50˚C to 300˚C, accuracy ±1˚C at 20˚C). The digital thermometer is calibrated against an ice water slurry bath at ˚C. Preparation of materials is performed at an environmental room temperature of 20˚C to 22˚C at one atmosphere.

4.1.2. Ice Inner Centrifuge Tube Preparation

Tap-water (20˚C to 22˚C) was used as the starting material. Given the degree of uncertainty produced by small size [9] [11] the ice volume is scaled up to 20 ml which is then transferred into a acrylic (sometimes called, plexiglass or clear polystyrene) tube (thermal conductivity ~0.14 W cm^2 [61], with dimensions of 1.2 × 2 × 11 cm) which was placed in a domestic freezer over night at −17˚C to −18˚C.

Once taken out of the freezer and placed at room temperature with accumulated frost removed from the outer surface of the tube, the ice was found to have a typical top surface temperature of 0˚C (8˚C outside surface temperature) after 2 minutes.

4.1.3. Ice Bath Preparation

Commercially bought ice cubes were used as the starting material. Given the degree of uncertainty as to the quantity of ice and the size of ice cubes used [12] [13], this work uses an irregular ice cube size with a diameter of approximately 1 cm^{-3} [62]. A dry Pyrex glass beaker (diameter = 4.3 cm, height = 6 cm) with thermal conductivity ~1 $W{\cdot}cm^{2}$ [61] is placed on a set of digital weigh scales and zeroed. The crushed is ice poured in and the beaker weighed again. One quotient of 50 g of crushed ice is then transferred to Pyrex glass Petri dish (diameter = 10.4 cm, height = 2 cm) with a thermal conductivity ~1 $W{\cdot}cm^{2}$ [61]. The process is repeated twice to fill 100 g of ice is into another Pyrex glass Petri dish. Using this method, after one minute at room temperature the packed ice has typical temperature of 0˚C.

4.1.4. Ice Water Bath Preparation

For the double bath experiments, commercially bought ice cubes are used as starting material then crushed to an approximate size of 1 cm^{-3} particles. The ratio of ice to water is initially fixed by the following method. A dry Pyrex glass beaker is placed on a set of digital weigh scales and zeroed. The crushed ice is then poured in and packed to a level of 50 ml and weighed, followed by tap-water to the same level. Using this method, it is found that 32 g of ice to 32 of water (ratio of 1:1 by weight) is obtained with a typical body temperature of 0˚C (3.5˚C outside surface temperature) after 1 minute at room temperature. The process repeated twice and the 50 ml ice water slurry is poured to a dry Pyrex glass Petri dish.

4.1.5. Water Dummy-Load Bath Preparation

Stock tap-water was stored in I L volumes within a domestic refrigerator. As and when required, four glass Pyrex beakers where filled with 50 ml of the stock tap-water and placed on the ovens glass carousel for use as water dummy-load. After preparation time, (directly before microwave illumination) the water dummy-load temperature was measured to be 8.5˚C ± 1˚C.

4.2. Lent Heat Control Experiments at Room Temperature (20˚C to 22˚C)

To investigate the underlying heat pathways of the internal ice bath, and external ice and crushed ice water baths a series of control experiments were designed and undertaken. The experiments were designed to measure the bath ice melt end-time as a function of vessel material (acrylic and Pyrex glass), and vessel geometry (beaker and Petri dish). The thermal heat transfer was calculated as the mass of ice multiplied by the Latent heat of fusion (334 $J{\cdot}g^{-1}$ at 0˚C). The rate of energy transfer (W) is estimated by dividing the thermal heat transfer value by

the melt end-time (measured in seconds). At the end of all the ice melt end-time experiments the finished water temperatures were measured to be 3˚C ± 0.5˚C.

Table 3 shows that the ice and crushed S/R/ ratio [57] in relation to the rate of thawing of ice at room temperature. For the amount of ice used here, the room temperature thaw time is some 100 greater than the microwave thaw times. Under these conditions the estimated power consumed is of the order of 1.6 W for the tube-in-tube, 3.8 w for the beaker and 8 to 9.5 W for the Petri dish system.

4.3. Single Ice Bath Microwave Irradiation Experiments

The reconstruction of the internal ice bath (tube-in-tube) experiments [9] [10] used six inner tubes filled with 20 lm of frozen water and placed in an outer 50 ml polypropylene tube containing 10 lm of the pseudo-suspension. Each tube-in-tube system is then placed in a 50 ml beaker for support; the complete arrangement is placed at the center of the ovens glass carousel. Set-up time for this procedure is 1 minute with the suspension temperature cooled to 20˚C ± 5˚C. The arrangements are microwave irradiated at a power level of 55 % for individual times 0 to 45 s, in steps of 5 s with a temperature limit of 70˚C. Directly after microwave irradiation the pseudo-suspension temperature was measured and the ice condition recorded. The results are given as a solid line in Figure 6.

For the nested beaker-in-Petri dish, six Pyrex glass beakers containing 10 ml of 37˚C pseudo-suspension are placed in six Pyrex glass Petri dishes containing 100 g crushed ice, with the ice mean level 5 mm above the suspension level. For the floating beaker-in-Petri dish, sex Pyrex glass Petri dishes were filled with 100g of crushed iced. A beaker containing 10 ml of 37˚C pseudo-suspension is placed on top of the crushed ice. Each of the beaker-Petri dish systems were placed in the center of the ovens glass carousel with a set-up time of 1 minute

Table 3. Ice and ice water bath control latent heat of fusion data at 20˚C to 22˚C.

Bath system	S/V ratio (cm^{-1})	RT melt end-time (s)	Thermal heat transfer (J)	Estimated Watts (W)
20 g ice; tube-in-tube	33.6/22 ~1.5	4084 ± 0.20	6680	1.6
32 g crushed ice in 32 g water; beaker	108/50 ~2.16	2820 ± 0.15	10,688	3.8
32 g crushed ice in 32 g water; Petri dish	196/50 ~3.9	1120 ± 0.20	10,688	9.5
50 g crushed ice; Petri dish	228/50 ~4.94	2130 ± 30	16,700	7.8
100 g crushed ice; Petri dish	268/100 ~2.68	4170 ± 30	33,400	8

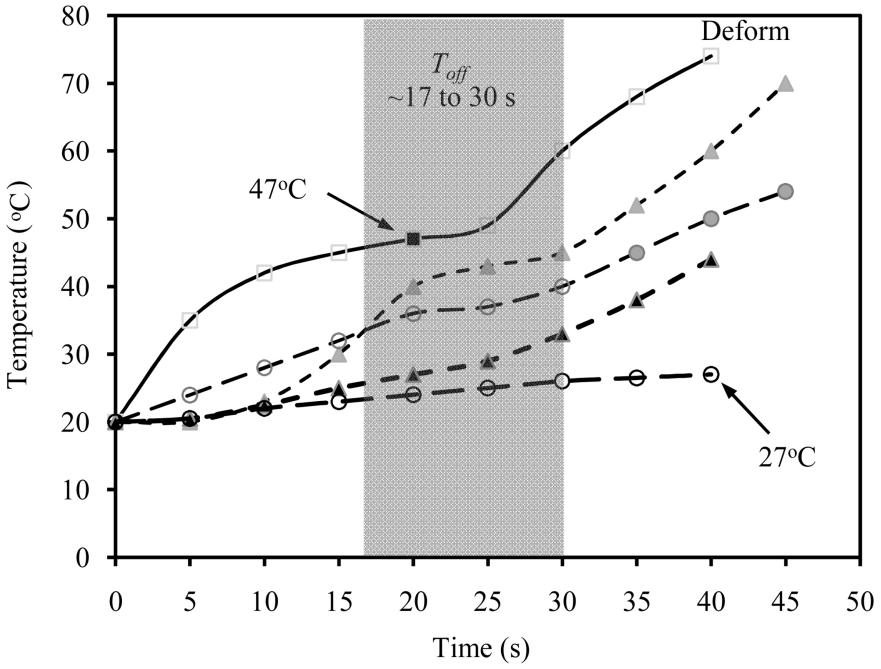

Figure 6. "Non-thermal" microwave-assisted (D = 55%) temperature profiles. Tube-in-tube: solid black line with open and closed squares. Nested beaker-in-Petri dish (short dashed line), and floating beaker (long dashed line with open circles) and gray denoting where beaker dropped into ice water slurry. Dummy-load with nested beaker-in-Petri dish (short dashed thick line, and black circles). Dummy-load with floating beaker-in-Petre dish (long dashed thick line with open circles).

that resulted in a cooled suspension temperature of 20˚C ± 5˚C. The systems are microwave irradiated at a power level of 55% for individual times of 0 to 45 s, in steps of 5 s. directly after microwave irradiation, the pseudo-suspension temperature is measured, and the crushed ice condition recorded. A maximum of twenty minutes between consecutive microwave experiments was allowed to minimize cavity-magnetron filament cold-start. The results for nestled (short dashed line) and floating (long dashed line) are given in **Figure 6** and **Figure 7**.

An additional series of experiment were performed to investigate the effect of a water dumpy-load (four beakers, each containing 50 ml tap-water at 10˚C). The dummy-loads where equally spaced around the circumference of the Petri dish. The results of nested and floating beaker-in-Petri dish with dummy-load are shown in **Figure 6**.

In the case of the tube-in-tube system (solid line) the profile exhibits the highest rate of temperature rise of the five profiles before reaching a temperature Plateau (47˚C at t = 20 s). At this timestamp the pseudo-suspension has a temperature of 13˚C (−20%) below the reported 1000 W bacteriophage suspension temperature [9]. Under these conditions, the Bluesky 800 W cavity-magnetron is operating in CW mode for the initial 17 seconds before the D = 55% setting turns off the cavity-magnetron power. Beyond the Plateau region the pseudo-suspension temperature reaches 70˚C at t = 40 s where the inner acrylic tube

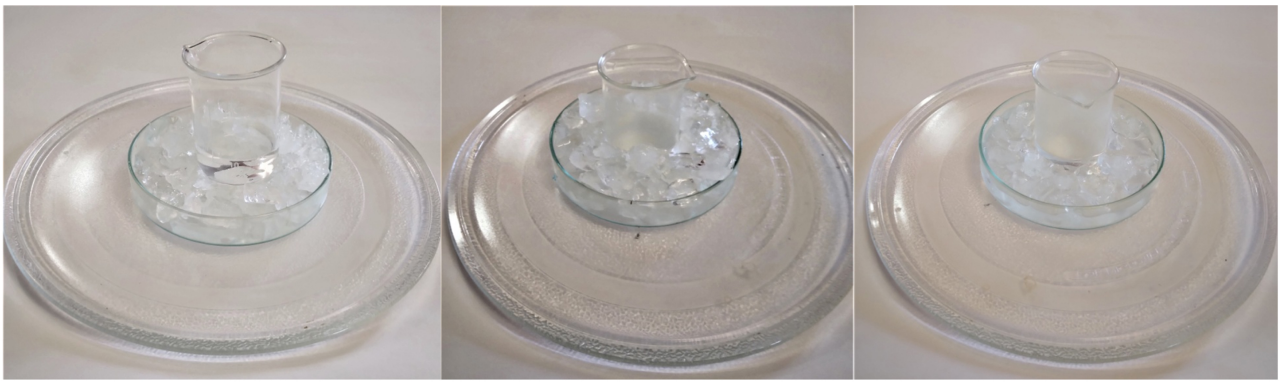

Figure 7. Photographs of the beaker-in-Petri dish system within the Bluesky microwave oven. Floating beaker on crushed ice (left), nested beaker in crushed ice (middle), and beaker in ice slurry (right). Microsoft filters have been used to enhance the glass and ice structures.

begins to thermal deform. Thus for the process time of $t = 20$ s, the 10 ml pseudo-suspension, has a total energy budget of 1.129 kJ and energy density of 0.112 kJ·ml^{-1}.

As regards to the nested (short dashed line) and floating (long dashed line) beaker-in-Petri dish and the profiles, each exhibit an initial low rate of temperature rise, with the nested beaker being the most retarded. After the Plateau region at $t = 40$ s the pseudo-suspension temperatures are 50˚C and 60˚C respectively, some 20˚C to 30˚C higher than that recorded by [12]. At $t = 40$ s the irradiation tine is 17 + 10 = 27 s which equate to a 10 ml pseudo-suspension total energy budget of 1.31 and 1.856 kJ with energy densities of 0.31 and 0.185 kJ·ml^{-1}.

The $D = 55\%$ dummy-load experiments produce a nested beaker pseudo-suspension temperature of 44˚C and a floating beaker suspension temperature of 27˚C at $t = 40$ s. In addition, each of the four separated dummy-loads increases in temperature from 10 to 15˚C. For the microwave irradiation time of $t = 17 + 10 = 27$ s these temperatures values equate to a 10 ml pseudo-suspension total energy budgets of 1 and 0.293 kJ, with energy densities of 0.1 and 0.0293 kJ·ml^{-1}. These would indicate that four separate dumpy-loads are directly absorbing the microwave energy that would have been otherwise absorbed by the pseudo-suspension. Moreover, the measured suspension temperature suggests that insufficient crushed ice water is used in non-dummy-load beaker experiments. This observation is partly apparent in **Table 2** where a 500 ml beaker filled with an unknown amount of ice is list [12]. Section 3.4 (double bath microwave experiments) uses this observation to inform a minimum of 200 mg of ice is used in the ice slurry bath for the double water bath experiments.

Associated with these suspension temperature curves, individual amounts of ice melt occurs **Table 4**. For the tube-in-tube system the melt ice collects at the bottom of the inner tube. At a $t = 20$ s the amount of melt water equates to approximately 6 ml, but the amount is difficult to ascertain due to the remaining

Table 4. "Non-thermal" microwave-assisted (D = 55%) as a function of irradiation time, t = 20 and 40 s. Measured melted ice for tube-in-tube system and beaker-Petri dish and beaker-in-Petri dish with dummy-load (DL).

Bath system	Irradiation time (s)	Melt water (ml)	Comments
Tube-in-tube	20	~6	Water poured slowly due ice blockage
Tube-in-tube	40	18 ± 1	Water poured quickly out of deformed tube
Floating beaker	20	30 ± 1	beaker at Petri dish floor at finish
Nested beaker	20	32 ± 1	beaker at Petri dish floor at start
Floating beaker	40	45 ± 5	beaker at Petri dish floor at finish
Nested beaker	40	45 ± 5	beaker at Petri dish floor at start
Floating beaker DL	20	11 ± 1	beaker on ice (no change)
Nested beaker DL	20	14 ± 1	beaker at Petri dish floor at start
Floating beaker DL	40	20 ± 1	beaker partially on ice
Nested beaker DL	40	25 ± 1	beaker at Petri dish floor at start

sold ice blocking the water flow out of the tube. For the floating beaker-in-Petre dish, this generates 30 ± 1 ml at t = 20 s and 45 ± 5 ml at t = 40 s. In the case of the 45 ± 5 ml ice phase change, the resulting ice water slurry cannot support the weight of beaker and its suspension causing the beaker to drop into the slurry. Typically, the drop occurs at t > 35 s: naturally there is no corresponding drop for nested beaker as it is already seating on Petri dish floor.

4.4. Double Bath System Microwave Oven Experiments

Given that Asay *et al.* (2008) [13] states that a "large bucket filled with ice water" is used to cool the *E. coli* suspension. In this work, 200 g of crushed ice within a Pyrex glass beaker (15 cm diameter × 6.5 cm high), with 200 ml of tap-water filling the space between the ice particles is used: with initial temperature of 0˚C. Within the ice water slurry bath is a 200 ml Pyrex glass dish containing 100 ml of tap-water at an initial temperature of 26˚C, and due to its total mass it seats at the bottom of the outer vessel with the slurry mixture displaced to the side. Floating within the water bath is a 50 ml beaker containing the 10 ml pseudo-suspension. To prevent the beaker from tipping over into the water bath, a plastic annular fixture (12 cm outer diameter, 6.5 cm inner diameter, 0.15 cm thick) is used to keep the beaker upright **Figure 8**. Both the water bath and

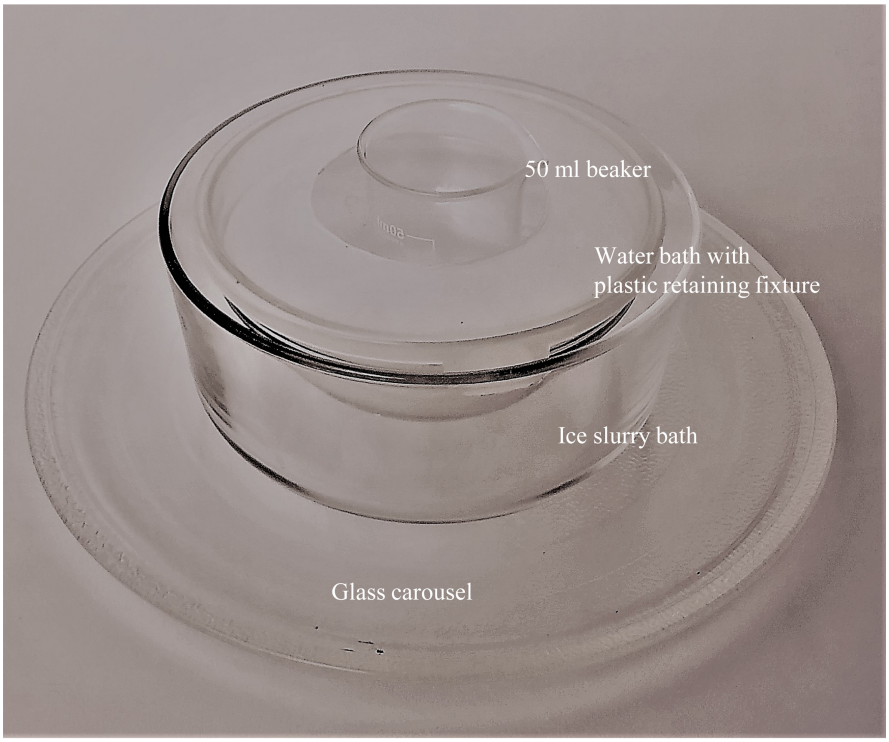

Figure 8. Photo of the dual bath vessels setup positioned on the microwave ovens glass carousel. Microsoft filters have been used to enhance the glass structure.

pseudo-suspension have an initial temperature of 26˚C thereby recreating the original conditions of minimal thermal shock to the *E. coli*. From the acoustic measurements in Section 3, a Bluesky cavity-magnetron D = 55% is chosen to simulate the Toshiba microwave oven power level of 5 out of 9 levels with an irradiation time of t = 20 and 40 s. Set-up time for this procedure is 1 minute and the final temperature measurements was also 1 minute. The results of these pseudo-suspension double bath experiments are given in **Table 5**.

Table 5 reveals that upon microwave irradiation the crushed ice within the ice water slurry bath does not melt at a constrain rate (82 g at 20 s and 104 g at 40 s) indicating the present of the D = 55% T_{off} period. Using a latent heat fusion value of 334 J·g^{-1} at 0˚C the energy absorbed in the respective microwave irradiation time periods (17 and 27 s) approximates to 26.72 and 33.4 KJ, respectively. In addition, the water bath temperature falls by approximately 2 and 5˚C during these respective irradiation time periods which approximates to 0.83 and 2 kJ lost to the crushed ice water slurry bath. Furthermore, the pseudo-suspension temperature increases by 0.5˚C and 1˚C respectively, or some 2 and 4.1 J.

Assuming that the Pyrex glass does not significantly adds to the power calculation, an estimation of the thermal power being delivered to the crushed ice process in the process time of 20 s (irradiation time 17 s) is 1.52 KW, some 1.9 time the rated power of the cavity-magnetron. Similar calculation for the process time of 40 s (irradiation time 27 s) yields 1.41 kW, some 1.7 times the cavity-magnetron rated power. The overestimated thermal power with respect to the

Table 5. Experimental results: 10 ml pseudo-suspension double bath at $D = 55\%$.

Bath, suspension	Initial temperature (˚C)	Temperature at 20 s (˚C)	Ice lost (g)	Temperature at 40 s (˚C)	Ice lost (g)
Crushed ice water slurry bath	0	1	80	1.5	100
Water bath	26	24		21	
Pseudo-suspension	26	26.5		27	

cavity-magnetron rated power may be expected due to the time in taking the temperature measurement the method of the calorimetric calculation. For the latter it is known that ice and liquid water will absorb energy at different rates in the T_{on} period. However, during the T_{off} period, the heated water transfers heat into the surrounding ice, such that in the following T_{on} period more water will be heated and will pass some of this heat on to ice in the following T_{off} period, and so on [2] [46] [56]. Thus the method of calculating the absorbed power used here will include heat transferred from the heated water in the T_{off} period. In addition, the presence of hotspots (regions of increased, focused, electric field strength) within the complex load particularly at the side of the water bath where the ice slurry is mainly located, will be heated at a greater rate than shielded volumes, such as the water bath and suspension bath.

5. Energy Phase-Space Projection and Electric Field Strength Analysis

This section describes the use of energy phase-space projection to map the "non-thermal" microwave-assisted 10 ml pseudo-suspension experiments, thereby allowing a direct comparison with the thermal microwave-assisted microorganism inactivation (≥4 $\log_{10}$) experiments present in **Figure 1**. The result of this mapping is given in **Figure 9**: with a horizontal-axis of 0 to 30 kJ, and a vertical-axis of 0 to 10 kJ·m^{-1}. The comparison thermal data corresponds to the 39 L Sharp microwave oven S630D rated at 1050 ± 50 W CW [16], and the 28 L Electrolux microwave oven ME28S rated at 900 W CW [51]. The ≥4 $\log_{10}$ inactivation microorganisms are Gram-negative vegetative *E. coli*, bacteriophage MS2 [16] and *Candida* spp. agar plated Petri dish [51].

The first feature of note in **Figure 9** is that the 10 ml "non-thermal" experiments data points are aligned on the 10 ml dotted trend-line, which is closely matched to the thermal microwave-assisted 10.93 m dashed trend-line. Within the "non-thermal" data set, the tube-in-tube system (x) outcome is positioned between the beaker-Petri dish with no dummy-load (+) and the beaker-Petri dish with dummy-load (o). The projection mapping also shows there is a clear experimental separation between the 10 ml and 10.93 and the 64 ml trend-line. This mapping resolution is sufficient to enable the 25 ml *Candida* spp. agar plated Petri dish data point to be displayed clearly.

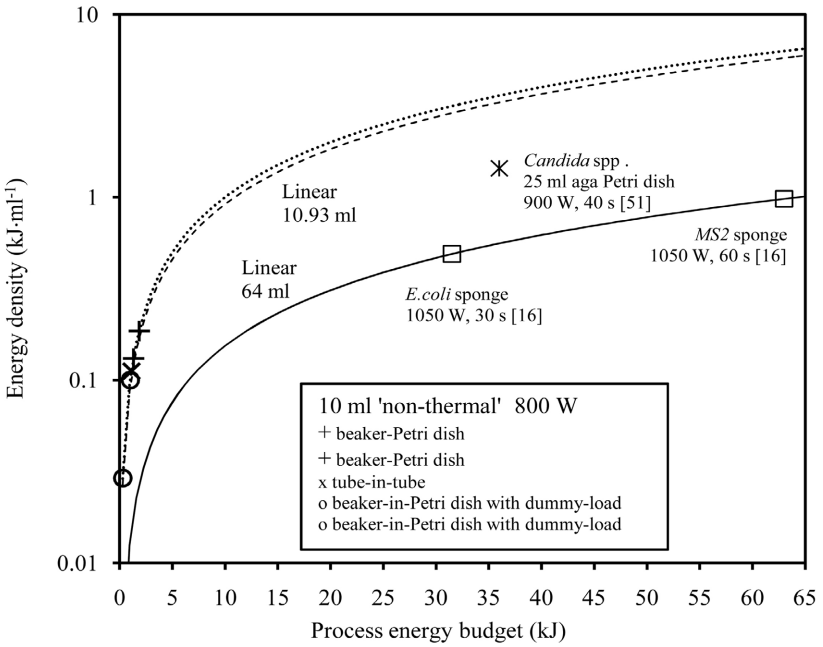

Figure 9. Energy phase-space projection (log-linear) for the "non-thermal" microwave-assisted heating of 10 ml pseudo-suspensions within beaker-Petri dish (+), tube-in-tube (x) and beaker-Petri dish with dummy-load (o): dotted line trend. Plus thermal' microwave-assisted ≥ 4 $\log_{10}$ inactivation of microorganism suspensions within different fomites (data taken from **Figure 1** [47]); Gram-negative vegetative *E. coli* 10.93 ml kitchen scrubbing pad (dotted-line) [16], 64 ml Gram-negative vegetative *E. coli* and bacteriophage MS2 sponge (□) [16], and 25 ml *Candida* spp. agar suspensions in Petri dish (star) [51].

The energy ranking for the "non-thermal" experiments may be rationalized by considering the geometry of the baths and dummy-load. Firstly the tube-in-tube system presents a narrow external vertical suspension column that is directly exposed to the microwave energy. This design feature is in contrast to the beaker-Petri dish systems where the suspension is surrounded by the crushed ice. Secondly the separated dummy-load (four 50 ml of crushed ice) that have lowest energy density values indicating that some of the applied 800 W is absorb directly by the dummy-loads themselves. These observations point to preferential volumetric heating of the suspension depending on whether an internal or external ice bath is employed. In the case of the internal ice bath, the suspension is directly illuminated, whereas the external ice bath suspension provides a shielding effect [50]. The absence of microwave irradiation in the duty cycle T_{off} period (where slow thermal conduction processes are present) induce a retardation of the suspension heating rate leading to a complex time-dependent suspension temperature profile, Rougier *et al.* (2014) [63], and Law and Dowling (2022) [46].

Electric Field Strength Estimation within the Energy Phase-Space Projection

It is generally claimed that "non-thermal" microwave-assisted effects arise from

the microwave electric field imposing a transmembrane electric potential. At low potentials hydrophobic nano diameter pores are reversibly generated that cause cell material leakage. Above a critical potential, however, membrane dielectric breakdown occurs causing an uncontrolled and irreversible cell material leakage, leading to cell lysis [5] [7] [9] [10] [11] [12] [24]. It is useful therefore to have an estimation of the instantaneous electric field strength (E, measured in $V \cdot m^{-1}$) within the microwave oven. From a dielectric volume heating perspective, the instantaneous microwave electrical absorbed power per unit volume (P_v, measured in $V \cdot m^{-3}$) is proportional electric field within the sample volume, (2) [2] [38] [39] [40] [55] [63] [64].

$$P_v \sim 2\pi f_o \varepsilon_o \varepsilon'' E_{rms}^2 \tag{2}$$

where $2\pi f_o \varepsilon_o \varepsilon''$ represents the effective dielectric conductivity (σ, measured in $S \cdot m^{-1}$), ε_o is the permittivity of free space (8.8542×10^{-12} $F \cdot m^{-1}$), ε'' is imaginary part of the complex permittivity of the load that decreases with temperature due to the increasing mobility of the water ionic component [36] [65] [66]. The E squared factor is derived that from the Ohms power Law ($P = GV^2$, where G is the inverse of R). Finally, the E_{rms} represents the root mean square of the electric field at the sample location. It is noted that there are a number variants of E in published literature, where the *rms* term is replaced by the effective square of the average electric field [2], or is removed and then dividing σ by 2 [38], or replacing E_{rms} with the E vector when spatiotemporal mapping of E [39] [40] [50] [55] and [63], and finally omitting the *rms* value, as it does not take in to account electromagnetic focusing, or hot spots within a multimode microwave oven [64].

Equation (2) however does require a knowledge of the tap-water ε'' value as a function of temperature, that may be found in published tables [64] and graphs [65]. In the case of graphs, digitalization software can be used to accurately reverse-engineer the visual information. For the "non-thermal" microwave-assisted Bluesky oven and thermal microwave-assisted Sharp oven data **Figure 8**, **Table 6** provides the calculated ε'', σ, and E_{rms} values.

Table 6. Imaginary part of the complex permittivity, conductivity, and E_{rms} at: 800 and 1050 ± 50 W at 2.45 GHz.

Suspension temperature	Tap-water (ε_r'')	σ ($S \cdot m^{-1}$)	Bluesky BMG20-8 E_{rms} at 800 W ($V \cdot m^{-1}$)	Sharp 630D E_{rms} at 1050 W ($V \cdot m^{-1}$)
Beaker-Petri dish dummy load ~27˚C	~12	~1.63	~22.1	-
Beaker-Petri dish ~40˚C	~7.5	~1.1	27	-
Tube-in-tube 47˚C	~6.9	~0.94	29.2	-
E. coli 83˚C ± 1˚C [16]	~3.6	~0.49	-	~46.2
MS2 85˚C ± 1˚C [16]	~3.2	~0.43	-	~49

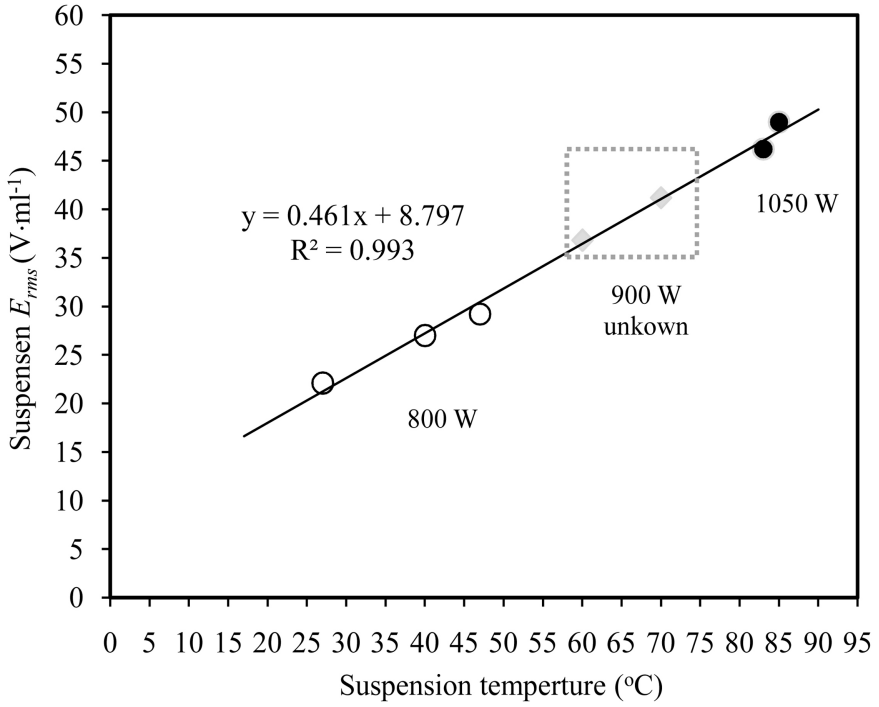

Figure 10. Suspension calibration for "non-thermal" 800 W microwave-assisted data points (o) and 1050 ± 50 W thermal microwave-assisted data points (•). Estimation of E_{rms} within the Electrolux 900 W (diamonds) inactivation process.

Table 7. Estimated ε'', σ and E_{rms} for *Candida*. app [51].

Electrolux 900 W	Temperature (˚C)	Suspension (ε_r'')	σ(S·m^{-1})	E_{rms} (V·m^{-1})
25 ml *Candida*. app	60 to 70	3.89 to 4.87	0.53 to 0.69	36.8 to 41.2

Figure 10 shows the suspension temperature (horizontal-axis) plotted against ε'' (vertical-axis), where the 5 point trend-line equates to y = 0.461x + 8.799 with an R^2 = 0.9933. Using this strong linear association between suspension temperature and E, it is reasonable to extrapolate between the 800 and 1050 W data points to find the unknown suspension temperature and E in the Electrolux 900 W 25 ml *Candida* app. experiments. The first step in this extract process is to assume the 900 W parameters lay on the initial trend-line (without altering R^2) and between the 800 and 1050 W dataset points. For a corresponding temperature range between 60˚C to 70˚C this yields an E_{rms} value of 36.8 to 41.2 V·ml^{-1}, see diamond points in **Figure 10**. The second step is to insert these values in to Equation (2) to obtain values for ε'' and σ **Table 7**.

6. Summary

Historical (2001 to 2008) [9]-[13] multimode microwave oven "non-thermal" microwave-assisted inactivation of microorganism experiments have been revi-

sited by reconstructing the experiments within a domestic microwave oven (Bluesky model BMG20-8). The outcome of reconstructed experiments are analyzed using thermodynamic and electrical engineering tools, and described with detailed text, diagrams, and photographs. A novel non-invasive acoustic measurement is used to access the ovens cavity-magnetron time-modulated waveform information (T_{on}, T_{off}, time-base, and duty cycle). Being non-invasive and using standard acoustic software, the measurement is easy to implement by non-electrical engineers. For an 800 W CW rated cavity-magnetron, the following experimental observations are noted:

1) The cavity-magnetron warm-up period (3 to 4 s) can influence output power within the initial base-time period, typically 30 s of the process time. For example, where a selected process time of 20 s [9] [10], or 40 s [11] [12] and [13] > twice the base-time, the cavity-magnetron CW rated power multiplied by the microwave illuminated time may provide a more accurate value when calculating the process energy budget, rather than averaged duty cycle power (supplied by the manufacture) multiplied by the process time.

2) It is noted that an internal ice bath [8] [10] result in the suspension being directly exposed to microwave illumination, whereas an external ice bath [11] [12] [13] provide a degree of shielding [50] that retards the time-dependent heating profile.

3) Separated water dummy-loads isolate and control thermal heat transfer (conduction) to and from the suspension, thereby diverting a portion of the cavity-magnetron rated power away from the suspension.

4) Dual water bath reconstruction experiments with a minimum of 200 g of ice with a ratio 1:1 to tap-water is sufficient to stabilize a 10 ml suspension temperature between 26˚C to 27˚C. The experiments reveal a complex heat pathway between the crushed ice and water within an ice slurry bath. In addition between the ice slurry bath and the intermediate water bath, where the main heat absorbing element, or dummy-load, is the crushed ice slurry bath.

5) Energy phase-space projection has been employed to analysis the "non-thermal" microwaves-assisted information. This approach enables the data to be directly compared with thermal microwave-assisted data. For close neighborhood data (800 to 1050 ± 50 W, and 10 ml to 64 ml suspension volumes, comparative values of E_{rms} have been calculated (22 to 41.2 $V \cdot m^{-1}$).

6) It is noted that multiplying E_{rms} by factor of 2.82 yields a peak-to-peak value. However, this would assume that the coherent sinusoidal wave in the cavity-magnetron TE_{10}-mode waveguide is the same in the ovens multimode cavity. This is not the case as the transverse electric (and magnetic) field structure becomes incoherent due to reflections from complex load and multiple reflections from the cavity wall influence the cavity auto-matching resonant frequency that is bounded by the free-running frequency bandwidth of the cavity-magnetron (2.45 ± 0.05 GHz).

The paper has highlighted number of dielectric volumetric heating issues that

would benefit from further investigation.

1) For "non-thermal" microwave-assisted inactivation of homogenous microorganism populations require a process time of 20 to 40 s, it would be useful to have detailed recording measurements of T_{on}, T_{off}, time-base, and suspension parameters (volume and temperature) that can be matched to scanning electron microscope, transmission electron microscope, or atomic force microscope imaging plus cell leakage analysis.

1) The use of energy phase-space projections combined with 3-dimasional computer modeling of the electric field strength within a complex load, as a function process time (0 to 40 s) may reveal real and not yet studied microwave induced thermodynamic and electromagnetic effects.

3) Such a multidiscipline investigation would advance the understanding of microwave-assisted induced cell membrane disruption that leads to cell lysis.

Conflicts of Interest

The authors declare they have no conflicts of interest.

References

[1] Spencer, P.L. (1950) Method of Treating Foodstuffs. US Patent 2,495,429.

[2] Vollmer, M. (2004) Physics of the Microwave Oven. *Physics Education*, **39**, 74-81. https://doi.org/10.1088/0031-9120/39/1/006

[3] Banik, S., Bandyopadhyay, S. and Ganguly, S. (2003) Bioeffects of Microwave—A Brief Review. *Bioresource Technology*, **87**, 155-159. https://doi.org/10.1016/S0960-8524(02)00169-4

[4] de la Hoz, A., Díaz-Ortiz, A. and Moreno, A. (2007) Review on Non-Thermal Effects of Microwave Irradiation in Organic Synthesis. *Journal of Microwave Power & Electromagnetic Energy*, **41**, 45-66. https://doi.org/10.1080/08327823.2006.11688549

[5] Janković, S.M., Milošev, M.Z. and Novaković, M.L.J. (2014) The Effects of Microwave Radiation on Microbial Cultures. *Hospital Pharmacology*, **1**, 102-108. https://doi.org/10.5937/hpimj1402102J

[6] Kozempel, M., Annous, B.A., Cook, R.C., Scullen, O.J. and Whiting, R.C. (1998) Inactivation of Microorganisms with Microwaves at Reduced Temperatures. *Journal of Food Protection*, **61**, 582-585. https://doi.org/10.4315/0362-028X-61.5.582

[7] Kozempel, M., Cook, R.C., Scullen, O.J. and Annous, B.A. (2000) Development of a Process for Detecting Non-Thermal Effects. Development of a Process for Detecting Nonthermal Effects of Microwave Energy on Microorganisms at Low Temperature. *Journal of Food Processing and Preservation*, **24**, 287-301. https://doi.org/10.1111/j.1745-4549.2000.tb00420.x

[8] Shazman, A., Mizrahi, S., Cogan, U. and Shimoni, E. (2007) Examining for Possible non-Thermal Effects during Heating in a Microwave Oven. *Food Chemistry*, **103**, 444-453. https://doi.org/10.1016/j.foodchem.2006.08.024

[9] Wang, A., Cheng, N., Liou, Y.T. and Lin, K. (2001) Inactivation of Bacteriophage by Microwave Irradiation. *Journal of Experimental Microbiology and Immunology*, **1**, 9-18.

[10] Baines, B. (2005) A Comparison of the Effects of Microwave Irradiation and Heat

Treatment of T4 and T7 Bacteriophage. *Journal of Experimental Microbiology and Immunology*, **7**, 57-61.

[11] Bryant, S., Rahmanian, R., Tam, H. and Zabetian, S. (2007) Effects of Microwave Irradiation and Heat on T4 Bacteriophage Inactivation. *Journal of Experimental Microbiology and Immunology*, **11**, 66-72.

[12] Barnett, C., Huerta-mounoz, U., James, R. and Pauls, G. (2006) The Use of Microwave Radiation in Combination with EDTA as an Outer Membrane Disruption Technique to Preserve Metalloenzyme Activity in *Escherichia coli*. *Journal of Experimental Microbiology and Immunology*, **9**, 1-5.

[13] Asay, B., Tebaykina, Z., Vlasova, A. and Wen, M. (2008) Membrane Composition as a Factor in Susceptibility of *Escherichia coli* c29 to Thermal and Non-Thermal Microwave Radiation. *Journal of Experimental Microbiology and Immunology*, **12**, 7-13.

[14] Tanaka, Y., Fujiwara, S., Kataoka, D., *et al.* (1998) Warming and Sterilizing Towels by Microwave Irradiation. *Yonago Acta Medica*, **41**, 83-88.

[15] Woo, I.S., Rhee, I.K. and Park, H.D. (2000) Differential Damage in Bacterial Cells by Microwave Radiation on the Basis of Cell Wall Structure. *Applied and Environmental Microbiology*, **66**, 2243-2247. https://doi.org/10.1128/AEM.66.5.2243-2247.2000

[16] Park, D.K., Bitton, G. and Melker, R. (2006) Microbial Inactivation by Microwave Radiation in the Home Environment. *Journal of Environmental Health*, **69**, 17-24.

[17] Fujikawa, H., Ushioda, H. and Kudo, Y. (1992) Kinetics of *Escherichia coli* Destruction by Microwave Irradiation. *Applied and Environmental Microbiology*, **58**, 920-924. https://doi.org/10.1128/aem.58.3.920-924.1992

[18] Orsini, M. and Romano-Spica, V. (2001) A Microwave-Based Method for Nucleic Acid Isolation from Environmental Samples. *Letters in Applied Microbiology*, **33**, 17-20. https://doi.org/10.1046/j.1472-765X.2001.00938.x

[19] Elhafi, G., Naylor, C.J., Savage, C.E. and Jones, R.C. (2004) Microwave or Autoclave Treatments Destroy the Infectivity of Infectious Bronchitis Virus and Avian Pneumovirus but Allow Detection by Reverse Transcriptase-Polymerase Chain Reaction. *Avian Pathology*, **33**, 303-306. https://doi.org/10.1080/0307945042000205874

[20] Cao, J.X., Wang, F., Li, X., *et al.* (2018) The Influence of Microwave Sterilization on the Ultrastructure, Permeability of Cell Membrane and Expression of Proteins of *Bacillus cereus*. *Frontiers in Microbiology*, **9**, 1870. https://doi.org/10.3389/fmicb.2018.01870

[21] Hong, S.M., Park, J.K. and Lee, Y.O. (2004) Mechanisms of Microwave Irradiation Involved in the Destruction of Fecal Coliforms from Biosolids. *Water Research*, **38**, 1615-1625. https://doi.org/10.1016/j.watres.2003.12.011

[22] Hayes, B.L. (2004) Recent Advances in Microwave-Assisted Synthesis. *Aldrichimica Acta*, **73**, 66-71.

[23] Hayes, B.L. and Collins, M.J. (2005) Reaction and Temperature Control for High Power Microwave-Assisted Chemistry Techniques. United States Patent US 6,917,023.

[24] Fregel, R., Rodríguez, V. and Cabrera, V.M. (2008) Microwave Improved *Escherichia coli* Transformation. *Letters in Applied Microbiology*, **46**, 498-499. https://doi.org/10.1111/j.1472-765X.2008.02333.x

[25] Wu, Y. and Yao, M. (2010) Inactivation of Bacteria and Fungus Aerosols Using Microwave Irradiation. *Journal of Aerosol Science*, **41**, 682-693. https://doi.org/10.1016/j.jaerosci.2010.04.004

[26] Wu, Y. and Yao, M. (2014) *In Situ* Airborne Virus Inactivation by Microwave Irradiation. *Chinese Science Bulletin*, **59**, 1438-1445. https://doi.org/10.1007/s11434-014-0171-3

[27] Perreux, L. and Loupy, A. (2001) A Tentative Rationalization of Microwave Effects in Organic Synthesis According to Reaction Medium and Mechanism Considerations. *Tetrahedron*, **57**, 9199-9223. https://doi.org/10.1016/S0040-4020(01)00905-X

[28] Loupy, A. and Rajender, S.V. (2006) Microwave Effects in Organic Synthesis: Mechanistic and Reaction Medium Considerations. *Chemistry Today*, **24**, 36-39.

[29] Wang, C., Hu, X. and Zhang, Z. (2019) Airborne Disinfection Using Microwave-Based Technology: Energy Efficient and Distinct Inactivation Mechanism Compared with Waterborne Disinfection. *Journal of Aerosol Science*, **137**, Article ID: 105347. https://doi.org/10.1016/j.jaerosci.2019.105437

[30] Heimbuch, B.K., Wallace, W.H., Kinney, K.R., *et al.* (2011) A Pandemic Influenza Preparedness Study: Use of Energetic Methods to Decontaminate Filtering Facepiece Respirators Contaminated with H1N1 Aerosols and Droplets. *American Journal of Infection Control*, **39**, e1-e9. https://doi.org/10.1016/j.ajic.2010.07.004

[31] Fisher, E.M., Williams, J.L. and Shaffer, R. (2011) Evaluation of Microwave Steam Bags for the Decontamination of Filtering Facepiece Respirators. *PLOS ONE*, **6**, e18585. https://doi.org/10.1371/journal.pone.0018585

[32] Lore, M.B., Heimbuch, B.K., Brown, T.L., Wander, J.D. and Hinrichs, S.H. (2012) Effectiveness of Three Decontamination Treatments against Influenza Virus Applied to Filtering Facepiece Respirators. *Annals of Occupational Hygiene*, **56**, 92-101.

[33] Zulauf, K.E., Green, A.B., Nguyen Ba, A.N., *et al.* (2020) Microwave-Generated Steam Decontamination of N95 Respirators Utilizing Universally Accessible Materials. *American Society Microbiology*, **11**, e00997. https://doi.org/10.1128/mBio.00997-20

[34] Pascoe, M.J., Robertson, A., Crayford, A., *et al.* (2020) Dry Heat and Microwave-Generated Steam Protocols for the Rapid Decontamination of Respiratory Personal Protective Equipment in Response to COVID-19-Related Shortages. *Journal of Hospital Infection*, **106**, 10-19. https://doi.org/10.1016/j.jhin.2020.07.008

[35] Law, V.J. and Dowling, D.P. (2021) MGS Decontamination of Respirators: A Thermodynamic Analysis. *GJRECS*, **1**, 1-17.

[36] Law, V.J. and Dowling, D.P. (2021) MGS Decontamination of Respirators: Dielectric Considerations. *GJRECS*, **1**, 6-21.

[37] Siddharta, A., *et al.* (2016) Inactivation of HCV and HIV by Microwave: A Novel Approach for Prevention of Virus Transmission among People Who Inject Drugs. *Scientific Reports*, **6**, Article No. 36619. https://doi.org/10.1038/srep36619

[38] Geedipalli, S.S.R., Rakesh, V. and Datta, A.K. (2007) Modeling the Heating Uniformity Contributed by a Rotating Turntable in Microwave ovens. *Journal of Food Engineering*, **82**, 359-368. https://doi.org/10.1016/j.jfoodeng.2007.02.050

[39] Yeong, S.P., Law, M.C., Lee, V.C.C. and Chan, Y.S. (2017) Modelling Batch Microwave Heating of Water. *IOP Conference Series: Materials Science and Engineering*, **217**, Article ID: 012035. https://doi.org/10.1088/1757-899X/217/1/012035

[40] Lee, G.L., Law, M.C. and Lee, V.C.C. (2020) Numerical Modelling of Liquid Heating and Boiling Phenomena under Microwave Irradiation Using OpenFOAM. *International Journal of Heat and Mass Transfer*, **148**, Article ID: 119096. https://doi.org/10.1016/j.ijheatmasstransfer.2019.119096

[41] Kubo, M.T.K., Siguemoto, E.S., Funcia, E.S., *et al.* (2022) Non-Thermal Effects of Microwave and Ohmic Processing on Microbial and Enzyme Inactivation: A Criti-

cal Review. *Current Opinion in Food Science*, **35**, 36-48. https://doi.org/10.1016/j.cofs.2020.01.004

[42] Gut, J.A.W. (2022) Response to "Non-Thermal Microwave Effects: Conceptual and Methodological Problems". *Food Chemistry*, **290**, Article ID: 133216. https://doi.org/10.1016/j.foodchem.2022.133216

[43] Jiao, X. and Fan, D. (2022) Letter to the Editor—Non-Thermal Microwave Effects: Conceptual and Methodological Problems. *Food Chemistry*, **372**, Article ID: 131217. https://doi.org/10.1016/j.foodchem.2021.131217

[44] Zhang, Z., Wang, J., Hu, Y. and Wang, L. (2022) Microwaves, a Potential Treatment for Bacteria: A Review. *Frontiers in Microbiology*, **13**, Article ID: 888266. https://doi.org/10.3389/fmicb.2022.888266

[45] Yap, T.F., Liu, Z., Shveda, R.A. and Preston, D.J. (2020) A Predictive Model of the Temperature-Dependent Inactivation of Coronaviruses. *Applied Physics Letters*, **117**, Article ID: 060601. https://doi.org/10.1063/5.0020782

[46] Law, V.J. and Dowling, D.P. (2022) Microwave Detection, Disruption, and Inactivation of Microorganisms. *American Journal Analytical Chemistry*, **13**, 135-161. https://doi.org/10.4236/ajac.2022.134010

[47] Law, V.J. and Dowling, D.P. (2022) Microwave-Assisted Inactivation of Fomite-Microorganism Systems: Energy Phase-Space Projection. *American Journal Analytical Chemistry*, **13**, 255-276. https://doi.org/10.4236/ajac.2022.137018

[48] Carpenter, S., Walker, B., Anderies, J.M. and Abel, N. (2001) From Metaphor to Measurement: Resilience of What to What. *Ecosystems*, **4**, 765-781. https://doi.org/10.1007/s10021-001-0045-9

[49] Cumming, G.S. and Collier, J. (2005) Change and Identity in Complex Systems. *Ecology and Society*, **10**, 29. https://doi.org/10.5751/ES-01252-100129

[50] Su, T., Zhang, W., Zhang, Z., Wang, X. and Zhang, S. (2022) Energy Utilization and Heating Uniformity of Multiple Specimens Heated in a Domestic Microwave Oven. *Food and Bioproducts Processing*, **132**, 35-51. https://doi.org/10.1016/j.fbp.2021.12.008

[51] Bazana, L.C.G., Carvalho, A.R., Mace, M. and Fuentefria, A.M. (2022) The Influence of the Microwave Oven on the Production of Solid Culture Medium and Quality of Microbial Growth. *Anais da Academia Brasileira de Ciências*, **94**, e20211104. https://doi.org/10.1590/0001-3765202220211104

[52] https://document.onl/documents/modulo1microondasme21s-me21g-me28s-me28g-me28xrev1.html?page=4

[53] Feinberg, A.E. (1968) Power Supply Circuit for Continuous Wave Magnetron Operated by Pulse Direct Current. US 3,396,342.

[54] Law, V.J. and Dowling, D.P. (2019) Chap. 14. Microwave Oven Plasma Reactor Modeling and Its Detection. In: 12*th Chaotic Modeling and Simulation International Conference*, *Springer Proceedings in Complexity*, Springer, Cham, 157-179. https://doi.org/10.1007/978-3-030-39515-5_14

[55] Houšová, J. and Hoke, K. (2002) Microwave Heating—The Influence of Oven and Load Parameters on the Power Absorbed in the Heated Load. *Czech Journal of Food Sciences*, **20**, 117-124. https://doi.org/10.17221/3521-CJFS

[56] European Standard (2011) Industrial Microwave Heating Installations. Test Methods for the Determination of Power Output. CSN EN 61307 ed. 3.

[57] Planinšič, G. and Vollmer, M. (2008) The Surface-to-Volume Ratio in Thermal Physics: From Cheese Cube to Physics to Animal Metabolism. *European Journal of*

Physics, **29**, 369-384. https://doi.org/10.1088/0143-0807/29/2/017

[58] Law, V.J., O'Neill, F.T. and Dowling, D.P. (2011) Evaluation of the Sensitivity of Electro-Acoustic Measurements for Process Monitoring and Control of an Atmospheric Pressure Plasma Jet System. *Plasma Sources Science and Technology*, **20**, Article ID: 035024. https://doi.org/10.1088/0963-0252/20/3/035024

[59] Law, V.J. and Dowling, D.P. (2022) "Dubro" Resophonic Guitar: Glissando Gestures. 14*th Chaotic Modeling and Simulation International Conference*, Athenes, 8-11 June 2021, 285-309. https://doi.org/10.1007/978-3-030-96964-6_20

[60] Law, V.J. (1998) Microwave Near-Field Plasma Probe. *Vacuum*, **51**, 463-468. https://doi.org/10.1016/S0042-207X(98)00199-7

[61] Maccus, S.M. and Blaine, R.L. (1994) Thermal Conductivity of Polymers & Glasses and Ceramics by Modulated DSC. *Thermochimica Acta*, **243**, 231-239. https://doi.org/10.1016/0040-6031(94)85058-5

[62] Yandori, M., Tsubotaa, Y. and Koroari, H. (1999) Fundamental Study of the Melting Process of Crushed Ice in Heat Storage Container. *Heat Transfer*, **28**, 583-596. https://doi.org/10.1002/(SICI)1523-1496(1999)28:7<583::AID-HTJ4>3.0.CO;2-W

[63] Rougier, C., Prorot, A., Chazal, P., Leveque, P. and Leprat, P. (2014) Thermal and Nonthermal Effects of Discontinuous Microwave Exposure (2.45 Gigahertz) on the Cell Membrane of *Escherichia coli*. *Applied and Environmental Microbiology*, **80**, 4832-4841. https://doi.org/10.1128/AEM.00789-14

[64] Law, V.J. and Denis, D.P. (2018) Domestic Microwave Oven and Fixed Geometry Waveguide Applicator Processing of Organic Compounds and Biomaterials: A Review. *Global Journal of Researches in Engineering*: *A Mechanical and Mechanics Engineering*, **18**, 1-10.

[65] Venkatesh, M.S. and Raghavan, G.S.V. (2004) An Overview of Microwave Processing and Dielectric Properties of Agri-Food Materials. *Biosystems Engineering*, **88**, 1-18. https://doi.org/10.1016/j.biosystemseng.2004.01.007

[66] Komarov, V.V. and Tang, J. (2004) Dielectric Permittivity and Loss Factor for Tap Water at 915 mhz. *Microwave and Optical Technology Letters*, **42**, 419-420. https://doi.org/10.1002/mop.20322